

Resolving the ϕ_2 (α) Ambiguity in $B \rightarrow \rho\rho$

J. Dalseno¹

¹*Instituto Galego de Física de Altas Enerxías (IGFAE),
Universidade de Santiago de Compostela, Santiago de Compostela, Spain*

Abstract

I propose an alternative method for measuring the CP violating phase ϕ_2 (α) without ambiguity in an extended $SU(2)$ isospin triangle analysis, which can ultimately be achieved by exploiting interference effects between $B^0 \rightarrow \rho^0 \rho^0$ and $B^0 \rightarrow a_1^\pm \pi^\mp$ in a time-dependent flavour-tagged amplitude analysis. Under certain assumptions on the effective ϕ_2 in each channel, I demonstrate with an idealised amplitude model that potential deviations to the tree-level CP violation parameters of $B^0 \rightarrow a_1^\pm \pi^\mp$ as would be induced by penguin contributions, is sufficiently high within current experimental uncertainties so as to accomplish this with Run 3 data at LHCb and easily at BelleII.

I. INTRODUCTION

Violation of the combined charge-parity symmetry (CP violation) in the Standard Model (SM) arises from a single irreducible phase in the Cabibbo-Kobayashi-Maskawa (CKM) quark-mixing matrix [1, 2]. Various processes offer different yet complementary insight into this phase which manifests in a number of experimental observables over-constraining the Unitarity Triangle. Decays that proceed predominantly through the $\bar{b} \rightarrow \bar{u}u\bar{d}$ tree transition (figure 1a) are sensitive to the interior angle of the Unitarity Triangle $\phi_2 = \alpha \equiv \arg(-V_{td}V_{tb}^*)/(V_{ud}V_{ub}^*)$. This phase can be accessed through mixing-induced CP violation observables measured from time-dependent, flavour-tagged analyses.

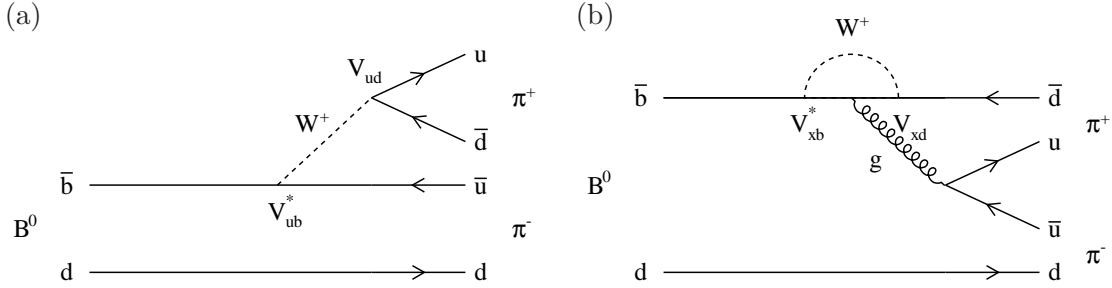


FIG. 1: Leading-order Feynman diagrams for $B^0 \rightarrow \pi^+\pi^-$ decays. (a) depicts the dominant first-order amplitude (tree) while (b) shows the second-order loop (penguin) diagram. In the penguin diagram, the subscript x in V_{xb} refers to the flavour of the intermediate-state quark ($x = u, c, t$).

The angle ϕ_2 has so far been constrained in multiple systems including $B \rightarrow \pi\pi$ [3–8], $\rho\pi$ [9, 10], $\rho\rho$ [11–17] and $a_1^\pm\pi^\mp$ [18–20] with an overall uncertainty of around 4° [21], however one of the salient features of the overall ϕ_2 combination is the presence of degenerate solutions within the range $[0, \pi]$. Up to the 2σ level, two solutions currently persist, while beyond this further solutions emerge.

In general, the extraction of ϕ_2 is complicated by the presence of interfering amplitudes that distort the experimentally determined value of ϕ_2 from its SM tree-level expectation. These effects primarily include $\bar{b} \rightarrow \bar{d}u\bar{u}$ strong loop decays (figure 1b), although isospin-violating processes such as electroweak penguins, π^0 - η - η' mixing and ρ^0 - ω - ϕ mixing can also play a role.

Despite such contamination, it is possible to at least remove the isospin-conserving component by invoking $SU(2)$ arguments. The original method considers the three possible charge configurations of $B \rightarrow \pi\pi$ decays [22]. In the case of strong penguins, a total isospin of $I = 1$ is not allowed by Bose-Einstein statistics, leaving only the possibility of $I = 0$ as the mediating gluon is an isoscalar. However, in the specific case of $B^+ \rightarrow \pi^+\pi^0$, the further limiting projection $I_3 = 1$ additionally rules out $I = 0$, thereby forbidding strong penguin contributions to this channel.

The complex $B^0 \rightarrow \pi\pi$ and $\bar{B}^0 \rightarrow \pi\pi$ decay amplitudes obey the isospin relations

$$A^{+0} = \frac{1}{\sqrt{2}}A^{+-} + A^{00}, \quad \bar{A}^{+0} = \frac{1}{\sqrt{2}}\bar{A}^{+-} + \bar{A}^{00}, \quad (1)$$

respectively, where the subscripts refer to the combination of pion charges. The decay amplitudes can be represented as triangles in the complex plane as shown in figure 2. As

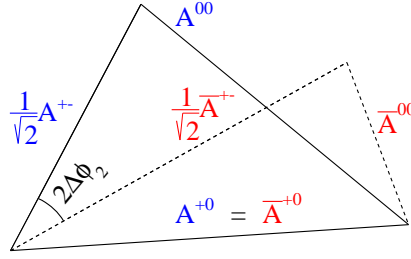


FIG. 2: Complex isospin triangles from which $\Delta\phi_2$ can be determined.

$B^+ \rightarrow \pi^+\pi^0$ is a pure tree mode, these triangles share the same base, $A_{+0} = \bar{A}_{+0}$, allowing $\Delta\phi_2$ to be determined from the phase difference between \bar{A}_{+-} and A_{+-} . These triangles and ϕ_2 can be constrained from the experimentally measured branching fractions, $\mathcal{B}(B^0 \rightarrow \pi^+\pi^-)$, $\mathcal{B}(B^0 \rightarrow \pi^0\pi^0)$ and $\mathcal{B}(B^+ \rightarrow \pi^+\pi^0)$, direct CP violation parameters, $\mathcal{A}_{CP}(B^0 \rightarrow \pi^+\pi^-)$ and $\mathcal{A}_{CP}(B^0 \rightarrow \pi^0\pi^0)$, and the mixing-induced CP violation parameter $\mathcal{S}_{CP}(B^0 \rightarrow \pi^+\pi^-)$. This method has an eightfold discrete ambiguity in the determination of ϕ_2 , which arises from the four triangle orientations about A_{+0} and the two solutions of ϕ_2 as $\mathcal{S}_{CP} = \sqrt{1 - \mathcal{A}_{CP}^2} \sin(2\phi_2 + 2\Delta\phi_2)$. In principle, the isospin triangle reflections can be resolved given a favourable measurement of $\mathcal{S}_{CP}(B^0 \rightarrow \pi^0\pi^0)$, leaving two overall solutions remaining. However, this would require an experimentally challenging vertex determination from the photons in the final state that have undergone pair production early enough in the detector material [23].

It was also pointed out soon afterwards that the ambiguity could be resolved in the $B^0 \rightarrow (\rho\pi)^0$ system alone without the need to involve the charged B modes [24], though of course this still can be done in an isospin pentagonal analysis if desired. By performing a time-dependent flavour-tagged amplitude analysis, the additional degrees of freedom afforded by the phase space allows the penguin contribution to be disentangled from the tree amplitudes through interference effects in the Dalitz Plot exposing a single solution for ϕ_2 . However at this point, the first-generation B factories have encountered some difficulty obtaining a meaningful constraint with this method due to statistical limitations. Therefore, it is worth investigating other possibilities to resolve the ϕ_2 ambiguity.

As the $B \rightarrow \rho\rho$ system currently dominates the precision on ϕ_2 with only a two-fold degeneracy arising due to the small penguin contribution which collapses the isospin triangles, I suggest a deeper investigation of the 4π final state. Now it has already been shown that a $B^0 \rightarrow (\rho\pi)^0$ -style analysis for $B^0 \rightarrow (a_1\pi)^0$ is not a viable approach as the charged and neutral a_1 resonances do not overlap in the phase space [25]. However, if a time-dependent flavour-tagged amplitude analysis of $B^0 \rightarrow \rho^0\rho^0$ could be performed instead of the procedure for measuring \mathcal{S}_{CP} that is currently in effect [15], the single solution obtained for the effective ϕ_2 could be sufficient to resolve the ϕ_2 ambiguity in the $B \rightarrow \rho\rho$ system with the extension to the isospin triangle analysis idea proposed in this paper.

The time-dependent decay rates of B^0 and \bar{B}^0 decays to a self-conjugate final state are given by

$$\begin{aligned}\Gamma(t) &\propto e^{-t/\tau}[(|A|^2 + |\bar{A}|^2) + (|A|^2 - |\bar{A}|^2) \cos \Delta m_d t - 2\Im(\bar{A}A^*) \sin \Delta m_d t], \\ \bar{\Gamma}(t) &\propto e^{-t/\tau}[(|A|^2 + |\bar{A}|^2) - (|A|^2 - |\bar{A}|^2) \cos \Delta m_d t + 2\Im(\bar{A}A^*) \sin \Delta m_d t],\end{aligned}\quad (2)$$

respectively, where A is the static decay amplitude, τ is the B^0 lifetime and Δm_d is the mass

difference between the B_H and B_L mass eigenstates. This form assumes no CP violation in the mixing $|q/p| = 1$, and that the total decay rate difference between the two mass eigenstates is negligible.

In the typical isobar approach, A can be written as the coherent sum over the number of intermediate states i , in the model as a function of 4-body phase space Φ_4 ,

$$A \equiv \sum_i a_i A_i(\Phi_4), \quad (3)$$

where a_i is a strong complex coupling determined directly from the data. Incorporating a complex CP violation parameter λ , for each contribution in the phase space, \bar{A} can be written as

$$\bar{A} \equiv \sum_i a_i \lambda_i \bar{A}(\Phi_4) = \sum_i a_i \lambda_i A(\bar{\Phi}_4), \quad (4)$$

where the phase space has been transformed under C and P conjugation, since A should only contain strong dynamics blind to flavour.

Now consider that current analyses have yet to find other significant contributions in the $B^0 \rightarrow \rho^0 \rho^0$ region, limiting interference opportunities. While there is no doubt these should emerge with increased statistics, they would roughly have to carry the phase ϕ_2 also. Furthermore, as only flavour-non-specific states may populate the phase space, it is clear from eq. 4 that the weak phase will more-or-less factorise out of the sum. Then in the absence of significant accompanying direct CP violation, this implies $\bar{A} \approx A \forall \Phi_4$, meaning that by the final term of eq. 2, the $\bar{A}A^*$ product will essentially be real-defined, indicating that two solutions would remain for the effective ϕ_2 . Indeed, this is the reason why a single solution for $\phi_1 = \beta \equiv \arg(-V_{cd}V_{cb}^*)/(V_{td}V_{tb}^*)$ cannot yet be found in the golden channel $B^0 \rightarrow K_S^0 K^+ K^-$, which is similarly lacking a flavour-specific intermediate state or significant direct CP violation otherwise.

It is difficult to envision that the penguin contribution of an amplitude already experimentally suppressed relative to $B^0 \rightarrow \rho^0 \rho^0$ can be so large as to prevent this scenario from occurring. However, by expanding the analysis phase space to include $B^0 \rightarrow a_1^\pm \pi^\mp$, I will demonstrate that the current experimental precision on its physics parameters provides a meaningful space for distortion of its weak phase and direct CP violation parameters from the tree-level expectations of ϕ_2 and null, respectively. These penguin-induced deviations in turn, allow for a unique determination of the effective ϕ_2 in $B^0 \rightarrow \rho^0 \rho^0$ through interference, with the amount of data expected to be collected by B physics experiments in the near future.

This paper is organised into 5 sections. In Section II, I outline the extension to the isospin triangle analysis that would allow a single solution for ϕ_2 to be obtained. Section III describes the rudimentary model used to generate pseudo-experiments interfering $B^0 \rightarrow \rho^0 \rho^0$ against $B^0 \rightarrow a_1^\pm \pi^\mp$. The results of the pseudo-experiment study are given for various experimental milestones in Section IV and finally conclusions are drawn in Section V.

II. EXTENSION TO THE ISOSPIN TRIANGLE ANALYSIS

I follow the general approach outlined by the CKMfitter Group given in ref. [21]. They describe 7 mostly independent observables which are related to the decay amplitudes as

$$\frac{1}{\tau_B^{i+j}} \mathcal{B}^{ij} = \frac{|\bar{A}^{ij}|^2 + |A^{ij}|^2}{2}, \quad \mathcal{A}_{CP}^{ij} = \frac{|\bar{A}^{ij}|^2 - |A^{ij}|^2}{|\bar{A}^{ij}|^2 + |A^{ij}|^2}, \quad \mathcal{S}_{CP}^{ij} = \frac{2\Im(\bar{A}^{ij} A^{ij*})}{|\bar{A}^{ij}|^2 + |A^{ij}|^2}, \quad (5)$$

where i, j represents the charge configuration of the intermediate ρ resonances and τ_B^{i+j} is the lifetime of the B^+ ($i + j = 1$) or B^0 ($i + j = 0$). For convenience, I also adopt the isospin representation of the amplitude system for function minimisation purposes as given in ref. [26],

$$\begin{aligned} A^{+0} &= \mu e^{i(\Delta - \phi_2)}, & \bar{A}^{+0} &= \mu e^{i(\Delta + \phi_2)}, \\ A^{+-} &= \mu a, & \bar{A}^{+-} &= \mu \bar{a} e^{2i\phi_2^{+-}}, \\ A^{00} &= A^{+0} - \frac{A^{+-}}{\sqrt{2}}, & \bar{A}^{00} &= \bar{A}^{+0} - \frac{\bar{A}^{+-}}{\sqrt{2}}, \end{aligned} \quad (6)$$

where a, \bar{a} and μ are real, positive parameters related to the magnitude of the decay amplitudes, while Δ is a relative strong phase. The weak phase $\phi_2^{+-} = \arg(\bar{A}^{+-} A^{+0*})/2$, embodies the shift in ϕ_2 caused by the penguin contamination. The experimental observables can then be related to these set of free parameters as

$$\begin{aligned} \mathcal{B}^{+0} &= \tau_{B^+} \mu^2, & \mathcal{B}^{+-} &= \tau_{B^0} \mu^2 \frac{a^2 + \bar{a}^2}{2}, \\ \mathcal{B}^{00} &= \tau_{B^0} \frac{\mu^2}{4} \left\{ 4 + a^2 + \bar{a}^2 - 2\sqrt{2}[a \cos(\phi_2 - \Delta) + \bar{a} \cos(\phi_2 + \Delta - 2\phi_2^{+-})] \right\}, \\ \mathcal{A}_{CP}^{+-} &= \frac{\bar{a}^2 - a^2}{\bar{a}^2 + a^2}, & \mathcal{S}_{CP}^{+-} &= \frac{2a\bar{a}}{\bar{a}^2 + a^2} \sin(2\phi_2^{+-}). \end{aligned} \quad (7)$$

Now I extend the method for $B^0 \rightarrow \rho^0 \rho^0$ by replacing the amplitude-squared-level \mathcal{A}_{CP}^{00} and \mathcal{S}_{CP}^{00} observables that would ordinarily be determined experimentally, with the proposed directly measured amplitude-level observables

$$|\lambda_{CP}^{00}| = \left| \frac{\bar{A}^{00}}{A^{00}} \right|, \quad \phi_2^{00} = \frac{\arg(\bar{A}^{00} A^{00*})}{2}. \quad (8)$$

Clearly, in the limit of vanishing penguin contributions and other isospin-breaking effects, $\phi_2^{+-} = \phi_2^{00} = \phi_2$.

These constructs now permit the isospin triangles and ϕ_2 to be constrained without ambiguity in principle. In this paper, I employ a Frequentist approach where a χ^2 is constructed comparing the above theoretical forms for the 7 observables with their experimentally measured counterparts. The $\Delta\chi^2$ across the range of ϕ_2 can then be converted into a p -value scan, assuming it is distributed with one degree of freedom, from which confidence intervals can be derived.

One issue to be aware of is that early attempts with this method may not necessarily lead to a measured ϕ_2^{00} that completely rules out the second solution by 5σ . Particularly if this is the case, the χ^2 profile of ϕ_2^{00} must be used instead of the usual assumption of Gaussian-distributed errors in the χ^2 sum. In order to better understand the impact of increasingly preferred solutions, a test is performed on the $B \rightarrow \rho\rho$ system with the final results obtained by the BaBar Collaboration for longitudinal polarisation [11, 13, 15]. For ϕ_2^{00} , I assume a χ^2 profile that consists of the sum of χ^2 terms for each solution, $\phi_2^{00} = 9^\circ$ and $\phi_2^{00} = 81^\circ$, calculated from the expression $\mathcal{S}_{CP}^{00} = \sqrt{1 - (\mathcal{A}_{CP}^{00})^2} \sin 2\phi_2^{00}$. The χ^2 distribution of the first solution, which is furthest from the SM, then receives a penalty equal to the square of the statistical separation between the two solutions. In practice however, this distribution would come from a likelihood scan of ϕ_2^{00} convolved with the systematic uncertainty. The resulting

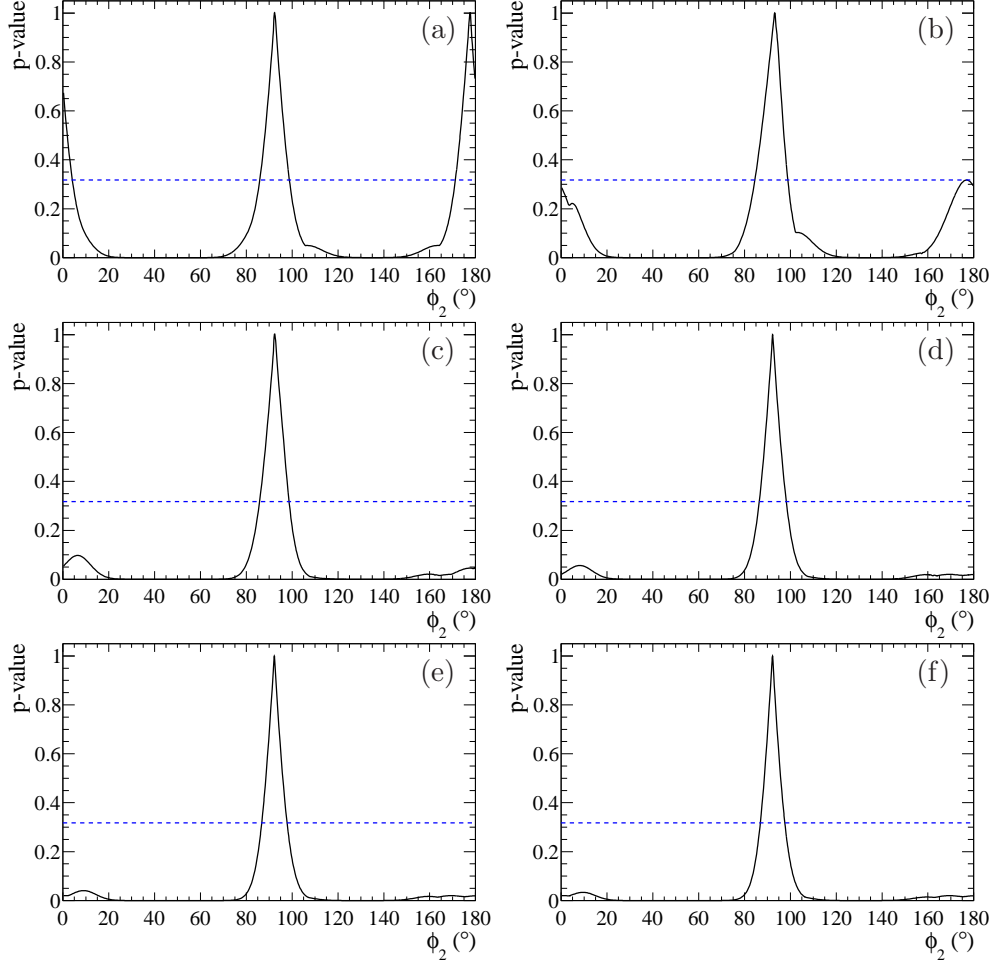


FIG. 3: p -value scans of ϕ_2 where the horizontal dashed line shows the 1σ bound. (a) shows the standard scan involving the quasi-two-body-parameters for $B^0 \rightarrow \rho^0 \rho^0$ obtained by the BaBar Collaboration. The remaining scans show the effects of increasing separation between the two solutions for ϕ_2^{00} from 1σ - 5σ , where their uncertainties are scaled to (b) $\delta\phi_2^{00} = 50.8^\circ$ (c) $\delta\phi_2^{00} = 25.4^\circ$ (d) $\delta\phi_2^{00} = 17.0^\circ$ (e) $\delta\phi_2^{00} = 12.7^\circ$ and (f) $\delta\phi_2^{00} = 10.2^\circ$.

ϕ_2 scans shown in figure 3 clearly demonstrate the potential of this proposed method to resolve solutions in $B \rightarrow \rho\rho$ if the $-2\log\mathcal{L}$ can differentiate between ϕ_2^{00} solutions, as measurements of \mathcal{S}_{CP}^{00} would otherwise result in all scans looking like figure 3a.

It is also instructive to understand the capacity to resolve solutions in ϕ_2 as a function of the central value of ϕ_2^{00} itself. In this test, I assume a single solution for ϕ_2^{00} can be resolved to 5σ with an uncertainty of 10° , however, I allow its central value to shift. The results shown in figure 4 illustrate that when the ϕ_2^{00} central value lies in the vicinity between the two solutions of ϕ_2 , which are mainly driven by the precision on \mathcal{S}_{CP}^{+-} , the resolution of its trigonometric ambiguity is not possible. If this proves to be a limiting factor in future analyses, an experimentally daunting amplitude analysis of $B^0 \rightarrow \rho^+ \rho^-$ would have to be the final resort in attempting to resolve a single solution in the $B^0 \rightarrow \rho\rho$ system.

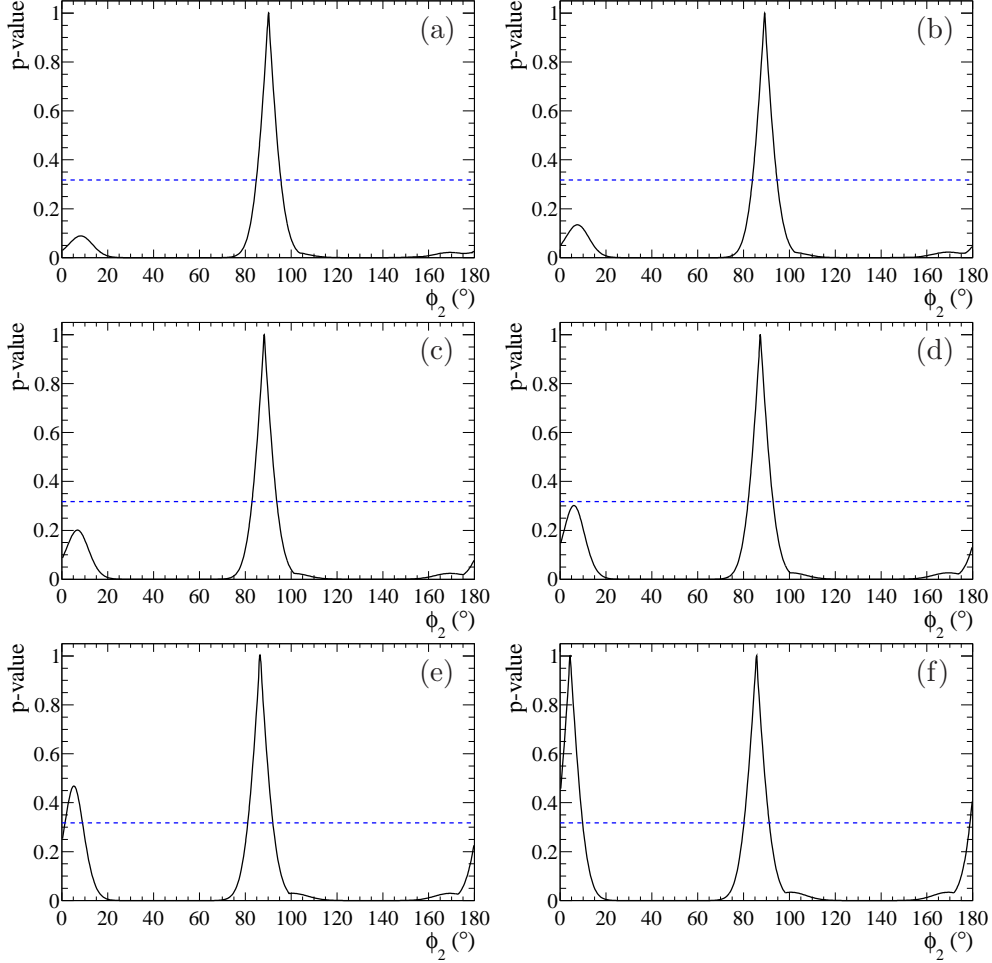


FIG. 4: p -value scans of ϕ_2 where the central value of ϕ_2^{00} is set to (a) $\phi_2^{00} = 70^\circ$ (b) $\phi_2^{00} = 65^\circ$ (c) $\phi_2^{00} = 60^\circ$ (d) $\phi_2^{00} = 55^\circ$ (e) $\phi_2^{00} = 50^\circ$ (f) $\phi_2^{00} = 45^\circ$. The horizontal dashed line indicates the 1σ bound.

III. TIME-DEPENDENT AMPLITUDE MODEL

Now that the possibility to constrain a single solution for ϕ_2 in $B \rightarrow \rho\rho$ is established under an ideal set of circumstances, it is important to estimate the feasibility of distinguishing between the two solutions of ϕ_2^{00} given the current experimental knowledge of the 4π final state. A primary concern regarding this proposed method is whether the hadronic uncertainties, particularly those arising from the a_1^\pm , can be controlled at a level that will still permit a clear distinction between the two solutions. Fortunately, parameters obtained from asymmetry measurements generally tend to be more immune to the effects of the model. However, in an attempt to provide a little more than just anecdotal evidence, I generate a set of pseudo-experiments varying the hadronic model within its current experimental uncertainties. I then set the yields to those expected at various milestones expected during the timelines of the BelleII and LHCb experiments and record the difference in $-2\log\mathcal{L}$ for each solution of ϕ_2^{00} obtained from a maximum likelihood fit to each pseudo-experiment. In any case, we only need sufficient precision to resolve a solution as most of the statistical power on the central value of ϕ_2 will come from $B^0 \rightarrow \rho^+\rho^-$. Experimental effects such as

detection efficiency, timing resolution and background contributions will be neglected in this study.

A. Amplitude Model

I consider a very rudimentary model with two contributions to the 4-body phase space coming only from the channels we know to exist, $B^0 \rightarrow \rho^0 \rho^0$ and $a_1^\pm \pi^\mp$. The amplitude for each intermediate state is parametrised as

$$A_i(\Phi_4) = B_{L_B}(\Phi_4) \cdot [B_{L_{R_1}}(\Phi_4)T_{R_1}(\Phi_4)] \cdot [B_{L_{R_2}}(\Phi_4)T_{R_2}(\Phi_4)] \cdot S_i(\Phi_4), \quad (9)$$

where B_{L_B} represents the production Blatt-Weisskopf barrier factor [27] depending on the orbital angular momentum between the products of the B^0 decays, L_B . Two resonances will appear in each isobar, denoted by R_1 and R_2 , for which respective decay barrier factors are also assigned. The Breit-Wigner propagators are represented by T , while the overall spin amplitude is given by S . Each isobar is Bose-symmetrised so that the total amplitude is symmetric under the exchange of like-sign pions.

The Blatt-Weisskopf penetration factors account for the finite size of the decaying resonances by assuming a square-well interaction potential with radius r . They depend on the breakup momentum between the decay products q , and the orbital angular momentum between them L . Their explicit expressions used in this analysis are

$$\begin{aligned} B_0(q) &= 1, \\ B_1(q) &= \frac{1}{\sqrt{1 + (qr)^2}}, \\ B_2(q) &= \frac{1}{\sqrt{9 + 3(qr)^2 + (qr)^4}}. \end{aligned} \quad (10)$$

In general, resonance lineshapes are described by Breit-Wigner propagators as a function of the energy-squared s ,

$$T(s) = \frac{1}{M^2(s) - s - im_0\Gamma(s)}, \quad (11)$$

where $M^2(s)$ is the energy-dependent mass and $\Gamma(s)$ is the total width which is normalised such that it represents the nominal width Γ_0 at the pole mass m_0 .

For the ρ^0 resonance, the Gounaris-Sakurai parametrisation is used to provide an analytic expression for $M^2(s)$ and $\Gamma(s)$ [28]. I ignore dispersive effects in the a_1^\pm , setting $M^2(s)$ to the pole mass. The energy-dependent width of the a_1^\pm is calculated from the integral of its Dalitz Plot as a function of s ,

$$\Gamma_{a_1^\pm}(s) = \frac{1}{2\sqrt{s}} \int |A_{a_1^\pm \rightarrow (\rho\pi)^\pm}(s)|^2 d\Phi_3. \quad (12)$$

where exclusive decay to $(\rho\pi)^\pm$ in an S -wave configuration and isospin symmetry i.e., $\Gamma_{a_1^\pm \rightarrow \rho^0 \pi^\pm}(s) = \Gamma_{a_1^\pm \rightarrow \rho^\pm \pi^0}(s)$ is also assumed. The form of the a_1^\pm energy-dependent width can be seen in figure 5.

Spin amplitudes are constructed with the covariant tensor formalism based on the Rarita-Schwinger conditions [29]. The spin S , of some state with 4-momentum p and spin projection

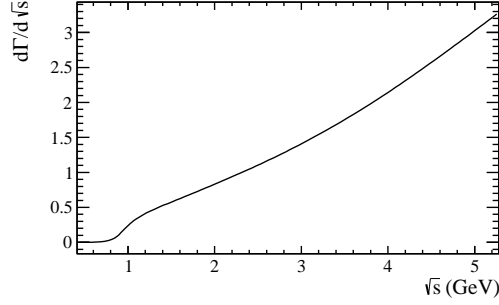


FIG. 5: Energy-dependent width of the a_1^\pm .

s_z is represented by a rank- S polarisation tensor that is symmetric, traceless and orthogonal to p . These conditions reduce the number independent elements to $2S + 1$ in accordance with the number of degrees of freedom available to a spin- S state. The sum over these polarisation indices of the inner product of polarisation tensors form the fundamental basis on which all spin amplitudes are built. Called the spin projection operator P , it has the capacity to project an arbitrary tensor onto the subspace spanned by the spin projections of the spin- S state.

Another particularly useful object is the relative orbital momentum spin tensor L , which for some process $R \rightarrow AB$, is the relative momenta of the decay products $q_R \equiv p_A - p_B$ projected to align with the spin of R ,

$$L_{\mu_1\mu_2\ldots\mu_L}(p_R, q_R) = P_{\mu_1\mu_2\ldots\mu_L\nu_1\nu_2\ldots\nu_L}(p_R) q_R^{\nu_1} q_R^{\nu_2} \cdots q_R^{\nu_L}. \quad (13)$$

Finally, to ensure that the spin amplitude behaves correctly under parity transformation, it is sometimes necessary to include the Levi-Cevita totally antisymmetric tensor $\epsilon_{abcs} p_R^d$. Each stage of a decay is represented by a Lorentz scalar obtained by contracting an orbital tensor between the decay products with a spin wavefunction of equal rank representing the final state.

Four topologies are necessary for this analysis. They include three for $B^0 \rightarrow \rho^0 \rho^0$ as S , P and D waves are permitted between the two ρ^0 resonances,

$$\begin{aligned} S : \quad & S \propto L_a(p_{\rho_1^0}, q_{\rho_1^0}) L^a(p_{\rho_2^0}, q_{\rho_2^0}), \\ P : \quad & S \propto \epsilon_{abcd} L^d(p_{B^0}, q_{B^0}) L^c(p_{\rho_1^0}, q_{\rho_1^0}) L^b(p_{\rho_2^0}, q_{\rho_2^0}) p_{B^0}^a, \\ D : \quad & S \propto L_{ab}(p_{B^0}, q_{B^0}) L^b(p_{\rho_1^0}, q_{\rho_1^0}) L^a(p_{\rho_2^0}, q_{\rho_2^0}). \end{aligned} \quad (14)$$

For $B^0 \rightarrow a_1^\pm \pi^\mp$, I only consider a single topology arising from the S -wave between the products of the a_1^\pm decay.

$$S \propto L_a(p_{B^0}, q_{B^0}) P^{ab}(p_{a_1^\pm}) L_b(p_{\rho^0}, q_{\rho^0}). \quad (15)$$

B. Pseudo-Experiment Generation Method

In order to get some early idea on the impact of hadronic and CP violating uncertainties on the ϕ_2^{00} measurement, I adopt a procedure of varying these within current experimental uncertainties for each pseudo-experiment. The average uncertainty on ϕ_2^{00} can then be

Parameter	Range	Reference
τ_{B^0}	1.520 ± 0.004 ps	[30]
Δm_d	0.5064 ± 0.0019 ps $^{-1}$	[30]
r	$[2, 6]$ c/GeV	-
$m_0(\rho^0)$	0.7690 ± 0.0009 GeV/ c^2	[30]
$\Gamma_0(\rho^0)$	0.1509 ± 0.0017 GeV	[30]
$\arg(a_{B^0 \rightarrow (\rho^0 \rho^0)_P})$	$[-180, +180]^\circ$	-
$ \lambda^{00} $	0.8	[15]
ϕ_2^{00}	81°	[15]
$m_0(a_1^\pm)$	1.225 ± 0.022 GeV/ c^2	[31]
$\Gamma_0(a_1^\pm)$	0.430 ± 0.039 GeV	[31]
$\arg(a_{B^0 \rightarrow a_1^+ \pi^-})$	$[-180, +180]^\circ$	-
$\phi_2(B^0 \rightarrow a_1^+ \pi^-)$	$(97.2 \pm 9.3)^\circ$	[19, 32]
$\phi_2(B^0 \rightarrow a_1^- \pi^+)$	$(107.0 \pm 16.9)^\circ$	[19, 32]
$\mathcal{A}_{CP}(B^0 \rightarrow a_1^\pm \pi^\mp)$	-0.06 ± 0.09	[19]
$\mathcal{C}_{CP}(B^0 \rightarrow a_1^\pm \pi^\mp)$	-0.01 ± 0.14	[19]
$\Delta \mathcal{C}(B^0 \rightarrow a_1^\pm \pi^\mp)$	$+0.54 \pm 0.13$	[19]
$\Delta \mathcal{S}(B^0 \rightarrow a_1^\pm \pi^\mp)$	-0.09 ± 0.15	[19]

TABLE I: Stage 1 parameters. Uncertainties indicate the parameter was Gaussian distributed, square brackets indicate uniform generation within the range while a single value is a constant of generation.

interpreted as the quadratic sum of the expected statistical error with the sources of model uncertainty considered in this analysis. The Monte Carlo (MC) is based on eq. 2 and requires a 2-stage process for generation. The first stage sets the model parameters of the $B^0 \rightarrow \rho^0 \rho^0$ and $B^0 \rightarrow a_1^\pm \pi^\mp$ isobars individually. A second stage is required to reverse engineer the complex couplings between them.

Table I records the generated parameters needed for stage 1. For $B^0 \rightarrow \rho^0 \rho^0$, the S and D -waves between the two ρ^0 mesons are practically indistinguishable in the phase space in stark contrast to D^0 decays, where the small size of phase space destroys some of the Bose-symmetry responsible for this degeneracy appearing in B^0 decays. This means that an amplitude analysis is only sensitive to the component of D -wave that is orthogonal to the S -wave, so the real part of the D -wave is fixed to zero as it will anyway be absorbed by the S -wave amplitude which is fixed along the real axis. The P -wave is completely distinguishable and so a random phase is assigned in this stage. The CP violation parameters of $B^0 \rightarrow \rho^0 \rho^0$ are shared between the 3 polarisations. I assume direct CP violation and a ϕ_2^{00} solution closest to the SM inferred by the BaBar measurement [15].

For $B^0 \rightarrow a_1^\pm \pi^\mp$, the relative phase to the fixed $B^0 \rightarrow \rho^0 \rho^0$ S -wave is unknown, so it is also assigned randomly in the first stage. Certain amplitude-level parameters can be derived from the quasi-two-body parameters listed in Table I, for which the Belle result is selected [19]. They include the relative magnitude of $B^0 \rightarrow a_1^- \pi^+$ compared to the dominant

Parameter	Range	Reference
$\mathcal{B}(B^0 \rightarrow \rho^0 \rho^0)$	$(0.95 \pm 0.16) \times 10^{-6}$	[33]
$f_L(B^0 \rightarrow \rho^0 \rho^0)$	0.745 ± 0.067	[17]
$f'_\parallel(B^0 \rightarrow \rho^0 \rho^0)$	0.5 ± 0.1	[17]
$f_S(B^0 \rightarrow \rho^0 \rho^0)$	$[0.5, 1.0][1 - f_P(B^0 \rightarrow \rho^0 \rho^0)]$	-
$\mathcal{B}(B^0 \rightarrow a_1^\pm \pi^\mp) \mathcal{B}(a_1^\pm \rightarrow \pi^\pm \pi^+ \pi^-)$	$(11.1 \pm 1.7) \times 10^{-6}$	[19]

TABLE II: Stage 2 parameters. Uncertainties indicate the parameter was Gaussian distributed while square brackets indicate uniform generation within the range.

$B^0 \rightarrow a_1^+ \pi^-$, which is given by

$$|a_{B^0 \rightarrow a_1^- \pi^+}| / |a_{B^0 \rightarrow a_1^+ \pi^-}| = \sqrt{\frac{1 - \Delta\mathcal{C}}{1 + \Delta\mathcal{C}}}, \quad (16)$$

and their relative phase difference given by

$$\arg(a_{B^0 \rightarrow a_1^- \pi^+} / a_{B^0 \rightarrow a_1^+ \pi^-}) = \arcsin(\Delta\mathcal{S}). \quad (17)$$

A coin-flip determines which solution for the relative phase is chosen in each pseudo-experiment.

The magnitude of the $B^0 \rightarrow a_1^\pm \pi^\mp$ CP violation parameters can also be determined from

$$|\lambda(B^0 \rightarrow a_1^\pm \pi^\mp)| = \sqrt{\frac{1 + A_\mp}{1 - A_\mp}}, \quad (18)$$

where

$$A_+ = \frac{\mathcal{A}_{CP} - \mathcal{C}_{CP} - \mathcal{A}_{CP}\Delta\mathcal{C}}{1 - \Delta\mathcal{C} - \mathcal{A}_{CP}\mathcal{C}_{CP}}, \quad A_- = -\frac{\mathcal{A}_{CP} + \mathcal{C}_{CP} + \mathcal{A}_{CP}\Delta\mathcal{C}}{1 + \Delta\mathcal{C} + \mathcal{A}_{CP}\mathcal{C}_{CP}}, \quad (19)$$

which represents the direct CP violation in $B^0 \rightarrow a_1^- \pi^+$ and $B^0 \rightarrow a_1^+ \pi^-$, respectively.

The remaining parameters are the effective ϕ_2 phases of the two $B^0 \rightarrow a_1^\pm \pi^\mp$ channels. These cannot be inferred from the quasi-two-body results obtained from existing time-dependent analyses. However, due to the remarkable agreement between the Belle result and the predictions from QCD factorisation [32], I select central values based on their theoretical prediction. The uncertainties in contrast, are taken from the Belle measurement which is sensitive to their algebraic average, inflated to reflect the size of $\Delta\mathcal{C}$, which is a measure of the relative difference in rates between $B^0 \rightarrow a_1^+ \pi^-$ and $B^0 \rightarrow a_1^- \pi^+$.

The remaining amplitude-level parameters are obtained in the second stage of parameter generation. As two strong phases were uniformly assigned in stage 1, their associated magnitudes have to be calculated. The imaginary part of the D -wave $B^0 \rightarrow \rho^0 \rho^0$ also needs to be determined as its real part is absorbed into the S -wave. These can be reverse-engineered from the parameters listed in Table II.

In order to generate the $B^0 \rightarrow \rho^0 \rho^0$ branching fractions for each polarisation, the combined branching fraction is first generated. I then take the LHCb measurement of the longitudinal and relative parallel polarisation [17] which immediately sets the P -wave fraction through

$$f_P(B^0 \rightarrow \rho^0 \rho^0) = [1 - f_L(B^0 \rightarrow \rho^0 \rho^0)] f'_\parallel(B^0 \rightarrow \rho^0 \rho^0), \quad (20)$$

Experiment	Milestone	Year	Effective Yield
LHCb	8 fb ⁻¹ (Run 2)	2018	1500
BelleII	10 ab ⁻¹	2021	6000
LHCb	23 fb ⁻¹ (Run 3)	2023	15000
BelleII	50 ab ⁻¹	2024	30000

TABLE III: Expected combined effective tagged yields of $B^0 \rightarrow \rho^0 \rho^0$ and $B^0 \rightarrow a_1^\pm \pi^\mp$.

according to the definition set by LHCb. For the remaining branching fractions of the S and D -waves, the split between them is uniformly generated where the S -wave is assumed to dominate.

To generate the branching fractions of $B^0 \rightarrow a_1^+ \pi^-$ and $B^0 \rightarrow a_1^- \pi^+$, the combined branching fraction is generated from the Belle result [19], where the relative amounts can be determined from parameters already generated in stage 1,

$$\mathcal{B}(B^0 \rightarrow a_1^+ \pi^-) \mathcal{B}(a_1^\pm \rightarrow \pi^\pm \pi^+ \pi^-) = \frac{1 + \Delta\mathcal{C} + \mathcal{A}_{CP}\mathcal{C}_{CP}}{2} \mathcal{B}(B^0 \rightarrow a_1^\pm \pi^\mp) \mathcal{B}(a_1^\pm \rightarrow \pi^\pm \pi^+ \pi^-). \quad (21)$$

The remaining 3 amplitude-level parameters of the model are then determined from a χ^2 fit relating the generated branching fractions for each isobar scaled to unity, to the fit fractions of each isobar calculated for the generated model in the 4-body phase space,

$$\mathcal{F}_i = \frac{\int (|A_i|^2 + |\bar{A}_i|^2) d\Phi_4}{\int \sum_i (|A_i|^2 + |\bar{A}_i|^2) d\Phi_4}. \quad (22)$$

C. Expected Yields

I generate pseudo-experiments based on individual amplitude-models with the `GENBOD` phase space function [34] and `qft++` to provide the spin densities [35]. Four tests are performed with crude estimates of the combined $B^0 \rightarrow \rho^0 \rho^0$ and $\mathcal{B}(B^0 \rightarrow a_1^\pm \pi^\mp)$ effective yields for 10 ab⁻¹ and the full 50 ab⁻¹ of data expected with BelleII, as well as the amount of data expected to be recorded by LHCb at the end of Run 2 and Run 3. These are recorded in Table III.

Belle found a combined total yield of around 1600 events [16, 19]. Neglecting efficiency differences and assuming improvements in selection arising from the widened phase space analysis region and better detector, a yield of around 90000 events should be realistic at BelleII. With a conservative estimate of 30% for the effective tagging efficiency, approximately 30000 effective signal events would remain.

Now, the crippling LHCb cut to reduce the $B^0 \rightarrow a_1^\pm \pi^\mp$ contributions to negligible levels led to a suppression of 50% of the $B^0 \rightarrow \rho^0 \rho^0$ signal [17]. This overlap region is critical to the method of attempting to extract a single solution for ϕ_2^{00} , thus I project a yield of 1000 $B^0 \rightarrow \rho^0 \rho^0$ events could be achieved by opening up the phase space to include $B^0 \rightarrow a_1^\pm \pi^\mp$ in Run 1. Again assuming similar detection efficiencies for $B^0 \rightarrow a_1^\pm \pi^\mp$, the combined yield would be near 12000 events. If Run 2 can achieve twice this yield, an effective tagging efficiency of 4% would leave an effective yield of around 1500 events. Run 3 is roughly estimated to procure an order of magnitude more data.

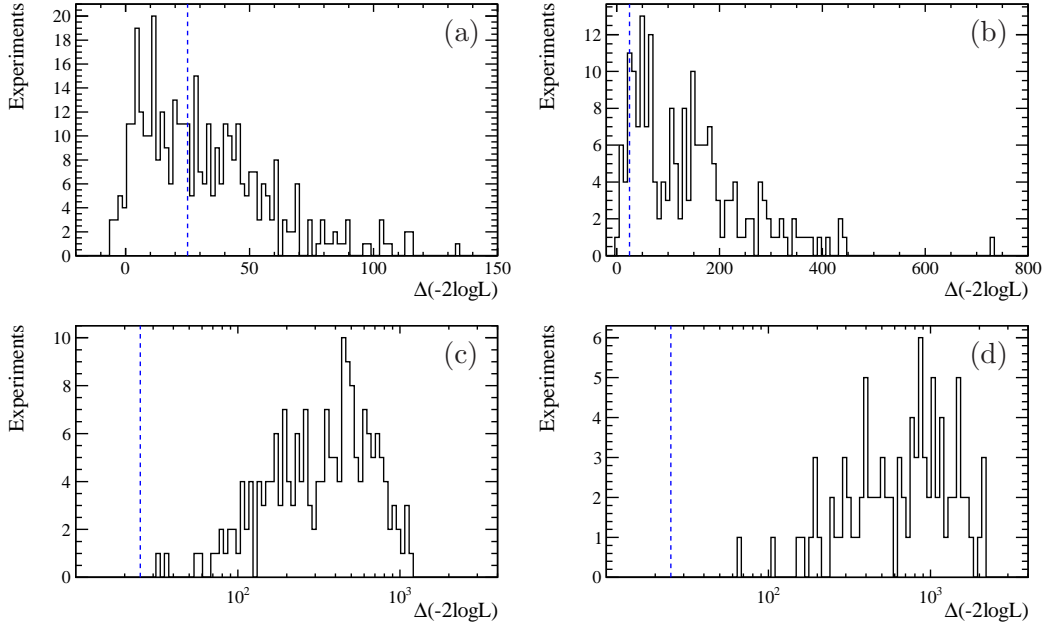


FIG. 6: Difference in $-2\log\mathcal{L}$ between the two solutions for ϕ_2^{00} expected with (a) Run 2 data at LHCb (b) 10 ab^{-1} at BelleII (c) Run 3 data at LHCb (d) 50 ab^{-1} at BelleII. The vertical dashed line indicates the cut-off at which a 5σ distinction is achieved. Note the log scale on the bottom plots.

IV. RESULTS

I then perform two fits to each pseudo-experiment. The first sets the starting value of ϕ_2^{00} to its generated value, the second sets it to the second solution. The distribution of the difference in $-2\log\mathcal{L}$ is then recorded in figure 6. The spread of these distributions is a measure of the statistical and specifically considered systematic effects at play in this study.

In the case of data recorded at LHCb up to the end of Run 2, a 2σ separation between ϕ_2^{00} solutions appears to be the most likely outcome. Corresponding to a scenario similar to that shown in figure 3c, this implies that a ϕ_2 solution could be ruled out at the 1σ level in $B \rightarrow \rho\rho$, which would already mark quite an important achievement. Due to the asymmetric nature of the log-likelihood difference, there is still over a 50% chance that the ϕ_2^{00} solutions could be resolved even at the 5σ level, at which point it will become important to improve measurements involving the other $B \rightarrow \rho\rho$ channels in order to further suppress multiple solutions for ϕ_2 . Under the assumptions laid out in this study, a 5σ separation between solutions would most likely be borderline with a data sample of 10 ab^{-1} collected by BelleII, while 50 ab^{-1} or Run 3 data from LHCb, should be more than adequate.

In the remaining, I consider additional scenarios that may be of interest. To highlight the impact of the LHCb Collaboration's suppression of the a_1^\pm , I repeat the study by imposing their condition that every 3-pion combination should have an invariant mass in excess of $2.1\text{ GeV}/c^2$ [17]. Figure 7a,b indicates that this would indeed constitute a risky venture at LHCb even at the end of Run 3, while at BelleII a clear separation of ϕ_2^{00} solutions is by no means assured with the full data set.

I also examine the situation when no CP violation is present in $B^0 \rightarrow \rho^0\rho^0$, with $|\lambda^{00}| = 1$ and $\phi_2^{00} = 88.8^\circ$, taken from the CKMfitter average for the direct measurement of ϕ_2 [21].

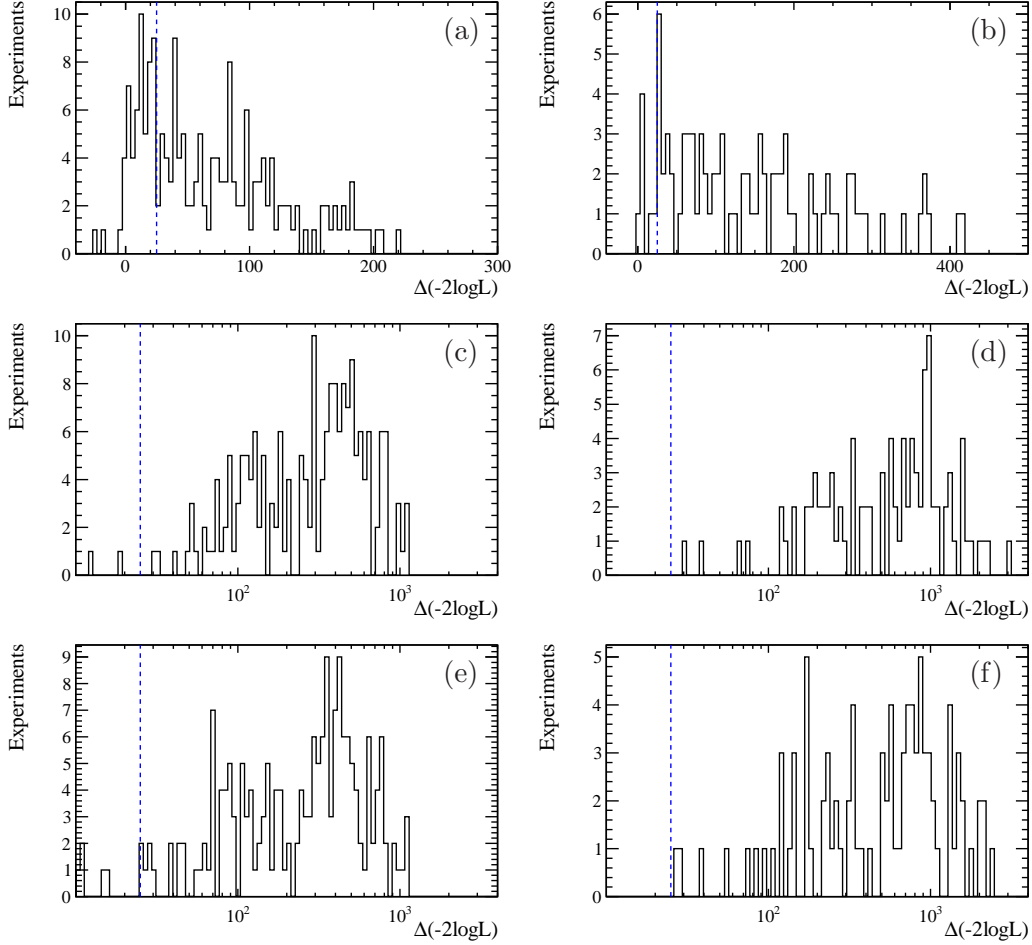


FIG. 7: Difference in $-2\log\mathcal{L}$ between the two solutions for ϕ_2^{00} expected with Run 3 data at LHCb shown on the left and 50 ab^{-1} at BelleII on the right. (a) and (b) represent the test with the LHCb a_1^\pm cut, (c) and (d) the case of no CP violation in $B^0 \rightarrow \rho^0\rho^0$, while in (e) and (f), ϕ_2^{00} is set to the $B^0 \rightarrow a_1^+\pi^-\pi^0$ weak phase. The vertical dashed line indicates the cut-off at which a 5σ distinction is achieved. Note the log scale on the bottom four plots.

Compared with the CP violating case shown in figure 6c,d, the absence of CP violation doesn't have an immediately obvious effect as portrayed in figure 7c,d. Finally, I track the difference in log-likelihood when ϕ_2^{00} exactly aligns with the generated weak phase of the dominant $B^0 \rightarrow a_1^+\pi^-\pi^0$ contribution. Again, no appreciable difference apart from perhaps a minor degradation in performance can be seen in figure 7e,f against the nominal case on display in figure 6c,d. These additional tests suggest that the ability to resolve ϕ_2^{00} solutions rests more on the presence of the $B^0 \rightarrow a_1^\pm\pi^\mp\pi^0$ amplitudes and their CP violation parameters rather than the CP violation parameters of $B^0 \rightarrow \rho^0\rho^0$ itself.

V. CONCLUSION

I present an extension to the $SU(2)$ isospin triangle analysis, that has the capacity to resolve the ϕ_2 degeneracy in the $B \rightarrow \rho\rho$ system under certain conditions. For this purpose a

time-dependent flavour-tagged amplitude analysis involving $B^0 \rightarrow \rho^0 \rho^0$ decays is proposed, where the phase space must be expanded over that used in current analyses to allow its interference with $B^0 \rightarrow a_1^\pm \pi^\mp$ to be sufficiently understood. If meaningful discrimination between the two solutions of the effective ϕ_2 in $B^0 \rightarrow \rho^0 \rho^0$ can be achieved and its central value is not located in the middle of the two solutions for the effective ϕ_2 coming from $B^0 \rightarrow \rho^+ \rho^-$, then the ϕ_2 solution degeneracy in $B \rightarrow \rho \rho$ can be resolved.

The current experimental uncertainty in $B^0 \rightarrow a_1^\pm \pi^\mp$ combined with a theoretical prediction of its own effective ϕ_2 , indicates that the benefits of potential deviation from tree-level expectations as would be induced by penguin contributions to these channels, are sufficient to warrant the additional experimental complications involved. Under varying assumptions on the CP violation present in $B^0 \rightarrow \rho^0 \rho^0$, the main hadronic uncertainties due to the a_1^\pm also appear to be under control as studies with roughly estimated signal yields at LHCb and BelleII indicate a real possibility to resolve ϕ_2 in the $B \rightarrow \rho \rho$ system at the end of Run 2 and with 10 ab^{-1} , respectively.

ACKNOWLEDGEMENTS

I am grateful to P. Vanhoefer for our discussions arising from his work on $B^0 \rightarrow \rho^0 \rho^0$ while I studied $B^0 \rightarrow a_1^\pm \pi^\mp$ at Belle, which inspired this idea. Thanks also goes out to J. Rademacker, whose pioneering methodology developed for 4-body Dalitz Plot analyses provided me with the knowledge necessary to evaluate the feasibility of this method. I am indebted to D. Martínez Santos and P. Naik for commenting on the paper draft and also to J. Albrecht who checked the projections on behalf of the LHCb physics coordination. Finally, special thanks to T. Gershon, whose careful reading improved this work immensely. This work was supported by XuntaGal (Spain).

-
- [1] N. Cabibbo, *Unitary Symmetry and Leptonic Decays*, *Phys. Rev. Lett.* **10** (1963) 531.
 - [2] M. Kobayashi and T. Maskawa, *CP Violation in the Renormalizable Theory of Weak Interaction*, *Prog. Theor. Phys.* **49** (1973) 652-657.
 - [3] BaBar collaboration, J.P. Lees et al., *Measurement of CP asymmetries and branching fractions in charmless two-body B-meson decays to pions and kaons*, *Phys. Rev. D* **87** (2013) 052009 [arXiv:1412.7254].
 - [4] Belle collaboration, J. Dalseno et al., *Measurement of the CP violation parameters in $B^0 \rightarrow \pi^+ \pi^-$ decays*, *Phys. Rev. D* **88** (2013) 092003 [arXiv:1302.0551].
 - [5] LHCb collaboration, R. Aaij et al., *Measurement of CP asymmetries in two-body $B_{(s)}^0$ -meson decays to charged pions and kaons*, *Phys. Rev. D* **98** (2018) 032004 [arXiv:1805.06759 (2018)].
 - [6] BaBar collaboration, B. Aubert et al., *Study of $B^0 \rightarrow \pi^0 \pi^0$, $B^\pm \rightarrow \pi^\pm \pi^0$, and $B^\pm \rightarrow K^\pm \pi^0$ decays, and isospin analysis of $B \rightarrow \pi \pi$ decays*, *Phys. Rev. D* **76** (2007) 091102 [arXiv:0707.2798].
 - [7] Belle collaboration, Y.-T. Duh et al., *Measurements of branching fractions and direct CP asymmetries for $B \rightarrow K \pi$, $B \rightarrow \pi \pi$ and $B \rightarrow K K$ decays*, *Phys. Rev. D* **87** (2013) 031103 [arXiv:1210.1348].
 - [8] Belle collaboration, T. Julius et al., *Measurement of the branching fraction and CP asymmetry in $B^0 \rightarrow \pi^0 \pi^0$ decays, and an improved constraint on ϕ_2* , *Phys. Rev. D* **96** (2017) 032007

- [arXiv:1705.02083].
- [9] BaBar collaboration, J.P. Lees et al., *Measurement of CP-violating asymmetries in $B^0 \rightarrow (\rho\pi)^0$ decays using a time-dependent Dalitz plot analysis*, *Phys. Rev. D* **88** (2013) 012003 [arXiv:1304.3503].
 - [10] Belle collaboration, A. Kusaka et al., *Measurement of CP Asymmetry in a Time-Dependent Dalitz Analysis of $B^0 \rightarrow (\rho\pi)^0$ and a Constraint on the Quark Mixing Matrix Angle ϕ_2* , *Phys. Rev. Lett.* **98** (2007) 221602 [hep-ex/0701015].
 - [11] BaBar collaboration, B. Aubert et al., *Study of $B^0 \rightarrow \rho^+\rho^-$ decays and constraints on the CKM angle α* , *Phys. Rev. D* **76** (2007) 052007 [arXiv:0705.2157].
 - [12] Belle collaboration, P. Vanhoefer et al., *Study of $B^0 \rightarrow \rho^+\rho^-$ decays and implications for the CKM angle ϕ_2* , *Phys. Rev. D* **93** (2016) 032010 [Erratum *ibid* **D 94** (2016) 099903] [arXiv:1510.01245].
 - [13] BaBar collaboration, B. Aubert et al., *Improved Measurement of $B^+ \rightarrow \rho^+\rho^0$ and Determination of the Quark-Mixing Phase Angle α* , *Phys. Rev. Lett.* **102** (2009) 141802 [arXiv:0901.3522].
 - [14] Belle collaboration, J. Zhang et al., *Observation of $B^\mp \rightarrow \rho^\mp\rho^0$ Decays*, *Phys. Rev. Lett.* **91** (2003) 221801 [hep-ex/0306007].
 - [15] BaBar collaboration, B. Aubert et al., *Measurement of the branching fraction, polarization, and CP asymmetries in $B^0 \rightarrow \rho^0\rho^0$ decay, and implications for the CKM angle α* , *Phys. Rev. D* **78** (2008) 071104 [arXiv:0807.4977].
 - [16] Belle collaboration, P. Vanhoefer et al., *Study of $B^0 \rightarrow \rho^0\rho^0$ decays, implications for the CKM angle ϕ_2 and search for other B^0 decay modes with a four-pion final state*, *Phys. Rev. D* **89** (2014) 072008 [Erratum *ibid* **D 89** (2014) 119903] [arXiv:1212.4015].
 - [17] LHCb collaboration, R. Aaij et al., *Observation of the $B^0 \rightarrow \rho^0\rho^0$ decay from an amplitude analysis of $B^0 \rightarrow (\pi^+\pi^-)(\pi^+\pi^-)$ decays*, *Phys. Lett. B* **747** (2015) 468-478 [arXiv:1503.07770].
 - [18] BaBar collaboration, B. Aubert et al., *Measurements of CP-Violating Asymmetries in $B^0 \rightarrow a_1^\pm(1260)\pi^\mp$ Decays*, *Phys. Rev. Lett.* **98** (2007) 181803 [hep-ex/0612050].
 - [19] Belle collaboration, J. Dalseno et al., *Measurement of branching fraction and first evidence of CP violation in $B^0 \rightarrow a_1^\pm(1260)\pi^\mp$ decays*, *Phys. Rev. D* **86** (2012) 092012 [arXiv:1205.5957].
 - [20] BaBar collaboration, B. Aubert et al., *Measurement of branching fractions of B decays to $K_1(1270)\pi$ and $K_1(1400)\pi$ and determination of the CKM angle α from $B^0 \rightarrow a_1(1260)^\pm\pi^\mp$* , *Phys. Rev. D* **81** (2010) 052009 [arXiv:0909.2171].
 - [21] J. Charles et al., *Isospin analysis of charmless B-meson decays*, *Eur. Phys. J. C* **77** (2017) no.8, 574 [arXiv:1705.02981].
 - [22] M. Gronau and D. London, *Isospin analysis of CP asymmetries in B decays*, *Phys. Rev. Lett.* **65** (1990) 3381.
 - [23] H. Ishino, M. Hazumi, M. Nakao and T. Yoshikawa, *New Measurements Using External Photon Conversion at a High Luminosity B Factory* [hep-ex/0703039].
 - [24] H.J. Lipkin, Y. Nir, H.R. Quinn and A. Snyder, *Penguin trapping with isospin analysis and CP asymmetries in B decays*, *Phys. Rev. D* **44** (1991) 1454.
 - [25] M. Gronau and J. Zupan, *Weak phase α from $B^0 \rightarrow a_1^\pm(1260)\pi^\mp$* , *Phys. Rev. D* **73** (2006) 057502 [hep-ph/0512148].
 - [26] M. Pivk and F.R. Le Diberder, *Isospin constraints from/on $B \rightarrow \pi\pi$* , *Eur. Phys. J. C* **39** (2005) 397-409 [hep-ph/0406263].
 - [27] F. von Hippel and C. Quigg, *Centrifugal-Barrier Effects in Resonance Partial Decay Widths, Shapes, and Production Amplitudes*, *Phys. Rev. D* **5** (1972) 624.

- [28] G.J. Gounaris and J.J. Sakurai, *Finite-Width Corrections to the Vector-Meson-Dominance Prediction for $\rho \rightarrow e^+e^-$* , *Phys. Rev. Lett.* **21** (1968) 244.
- [29] W. Rarita and J. Schwinger, *On a Theory of Particles with Half-Integral Spin*, *Phys. Rev.* **60** (1941) 61.
- [30] Particle Data Group, M. Tanabashi et al., *Review of Particle Physics*, *Phys. Rev. D* **98** (2018) 030001.
- [31] P. d’Argent and N. Skidmore et al., *Amplitude analyses of $D^0 \rightarrow \pi^+\pi^-\pi^+\pi^-$ and $D^0 \rightarrow K^+K^-\pi^+\pi^-$ decays*, *JHEP* **05** (2017) 143 [arXiv:1703.08505].
- [32] H.-Y. Cheng and K.-C Yang, *Hadronic charmless B decays $B \rightarrow AP$* , *Phys. Rev. D* **76** (2007) 114020 [arXiv:0709.0137].
- [33] HFLAV, Y. Amhis et al., *Averages of b-hadron, c-hadron, and τ -lepton properties as of summer 2016*, *Eur. Phys. J. C* **77** (2017) 895 [arXiv:1612.07233].
- [34] F. James, *Monte Carlo phase space*, CERN-68-15.
- [35] M. Williams, *Numerical object oriented quantum field theory calculations*, *Comp. Phys. Comm.* **180** (2009) 1847 [arXiv:0805.2956]; <https://github.com/jdalseno/qft>.